JACS
JOURNAL OF THE AMERICAN CHEMICAL SOCIETY

COMMUNICATION

pubs.acs.org/JACS

Hierarchical Helical Assembly of Conjugated Poly(3-hexylthiophene)-*block*-poly(3-triethylene glycol thiophene) Diblock Copolymers

Eunji Lee,[†] Brenton Hammer, Jung-Keun Kim, Zachariah Page, Todd Emrick,* and Ryan C. Hayward*

Department of Polymer Science and Engineering, University of Massachusetts, Amherst, Massachusetts 01003, United States

Supporting Information

ABSTRACT: We report on the solution-state assembly of all-conjugated polythiophene diblock copolymers containing nonpolar (hexyl) and polar (triethylene glycol) side chains. The polar substituents provide a large contrast in solubility, enabling formation of stably suspended crystalline fibrils even under very poor solvent conditions for the poly(3-hexylthiophene) block. For appropriate block ratios, complexation of the triethylene glycol side chains with added potassium ions drives the formation of helical nanowires that further bundle into superhelical structures.

Solution-processable conjugated polymers have received attention in recent years due to their potential for cost-effective, lightweight, and flexible electronics and photoactive materials.[1] Among π-conjugated polymers, polythiophene (PT) derivatives have been the most intensively studied as p-type active layer materials for thin-film organic solar cells and field effect transistors due to their high hole mobilities.[2] High-performance devices from such materials benefit from precise control of nanometer-scale morphology and molecular-scale crystallinity within the active components.[3] Thus, the control of thin-film morphology through self-assembly of rationally designed polymers is being pursued as a means to optimize performance.[2b] In the simplest case, placing aliphatic side chains on the PT backbone promotes solubility, enabling solution-state assembly into 1-D crystalline nanowires,[4] and also allowing electronic properties to be tuned as a function of side-chain length.[5] Such solution-processed nanostructures are attractive building blocks for fabricating thin-film devices, since they provide efficient intermolecular charge transport through crystalline domains without delicate thermal or solvent vapor annealing treatments.[6] The use of block copolymers, wherein a poly(3-alkylthiophene) (P3AT) block is covalently connected to another p-type polymer, an n-type polymer, or an insulating block, provides improved control over the self-assembled structures due to immiscibility or differences in crystallinity or solubility between the blocks.[7] However, the self-assembly of such polymers into crystalline nanostructures with precisely controlled shapes and sizes remains largely unexplored.

Here we describe the solution-state self-assembly of PT-based diblock copolymers, in which one PT block contains nonpolar side chains and the other PT block contains polar substituents. Specifically, we prepared regioregular poly(3-hexylthiophene)-*block*-poly(3-triethylene glycol thiophene) (P3HT-*b*-P3(TEG)T) diblock copolymers (Figure 1) that provide two distinct advantages for solution-state assembly. First, the large contrast in solubility between the blocks allows for the efficient formation of stably suspended crystalline nanostructures through addition of a poor solvent for P3HT, without the need to introduce a nonconjugated (i.e., photoinactive) solubilizing block. Second, the ability of the TEG side chains to complex alkali metal ions provides an additional handle to tune the hierarchical self-assembly of these conjugated polymers. These polymers give rise to nanowires upon addition of methanol to solutions of P3HT-*b*-P3(TEG)T in chloroform, with wire lengths that depend on block ratio and solvent quality. In addition, for appropriate block ratios, the presence of K^+ ions during self-assembly drives formation of helical wires that further bundle into superhelices containing two or more crystalline fibrils, as represented schematically in Figure 1 and described in detail below.

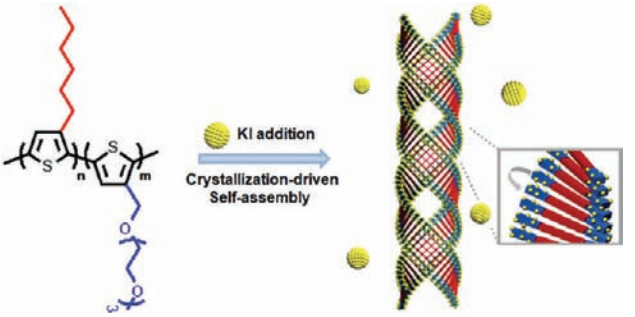

Figure 1. Molecular structure of P3HT-*b*-P3(TEG)T diblock copolymers and schematic representation of their assembly into superhelical structures through crystallization in the presence of potassium ions.

P3HT-*b*-P3(TEG)T diblock copolymers were synthesized following the procedure of McCullough and co-workers (Scheme S1).[8] The P3HT block was prepared by Grignard metathesis (GRIM) polymerization (using Ni(dppp)Cl_2) to give P3HT with a living chain-end, which was chain-extended into the diblock structure using the TEG-substituted thiophene monomer. The resulting products were purified by sequential Soxhlet extraction using methanol, hexane, and chloroform, respectively. Three diblock copolymers were studied in detail, having similar overall molecular weights but different targeted P3HT:P3(TEG)T weight ratios of 1:1, 2:1, and 4:1, denoted **H1T1**, **H2T1**, and **H4T1**, respectively. The actual ratios of the block lengths determined by ^{1}H NMR spectroscopy, and the polystyrene-equivalent molecular weights estimated by gel permeation chromatography (GPC) using chloroform as the eluent, are shown in Table 1.

In general, self-assembly of P3HT into crystalline nanowires can be achieved by addition of a nonsolvent to a polymer solution

Received: April 26, 2011
Published: May 31, 2011

dx.doi.org/10.1021/ja2038547 | *J. Am. Chem. Soc.* 2011, 133, 10390–10393

Table 1. Characteristics of P3HT-*b*-P3(TEG)T Polymers

polymer type	P3HT:P3(TEG)T weight ratio[a]	M_n (g·mol^{-1})[b]	PDI[b]
H1T1	1.0:1	18 000	1.7
H2T1	2.2:1	16 000	1.7
H4T1	4.0:1	18 000	1.5

[a] Determined from ^{1}H NMR. [b] Estimated by GPC.

in a good solvent.[6b,9] Here, the P3HT-*b*-P3(TEG)T polymers were initially dissolved in chloroform, a good solvent for both blocks. Aggregation was induced by addition of methanol, a selective solvent for P3(TEG)T, as indicated by a color change of the solution from orange to purple and confirmed by UV−vis and photoluminiscence (PL) spectroscopy. For example, the absorption spectrum of **H2T1** in chloroform exhibited a single peak, with a maximum at 450 nm, similar to dissolved P3HT in solution.[10] However, increasing methanol content in solution gave UV−vis spectra with a progressive decline in absorption at 450 nm and growth of vibronic bands at 515, 550, and 600 nm, indicative of interchain $\pi-\pi$ interactions associated with semicrystalline aggregate formation (Figure 2a).[5a,11] The isosbestic point at 502 nm indicates the presence of two distinct species, i.e., isolated **H2T1** chains and aggregates. The PL spectrum of **H2T1** revealed a progressive quenching of photoluminescence with increasing methanol content in the chloroform/methanol mixture, further confirming polymer aggregation (Figure S2a).[11a,12]

Dynamic light scattering (DLS) performed on **H2T1** solutions in chloroform/methanol mixtures provided further understanding of these structures, as analyzed using the CONTIN method. In a 19:1 chloroform/methanol mixture, a narrow size distribution with an average hydrodynamic diameter of 8 nm (Figure 2b) was observed, consistent with the large majority of chains being well dissolved. However, the weak vibronic bands in the UV−vis spectrum (Figure 1a) suggest that a small fraction of aggregates are present at this composition. As the methanol content increased, clear bimodal size distributions developed, indicating coexistence of dissolved P3HT-*b*-P3(TEG)T and larger aggregates.[13] The peak diameter of the aggregates increased from 78 to 342 to 531 nm for chloroform/methanol ratios of 9:1, 7:1, and 4:1, respectively, indicating a progressive growth in aggregate size.

Structural examination of **H2T1** aggregates was performed by transmission electron microscopy (TEM) on samples cast from 1 mg/mL solutions. At a 19:1 chloroform/methanol ratio, self-assembly of **H2T1** gave only short nanofibers, with lateral dimensions of 14−16 nm and lengths of a few hundred nanometers (Figure 2c). As anticipated on the basis of the UV−vis and DLS results, further addition of methanol drives the formation of longer nanofibers with lengths of several micrometers for a 4:1 solvent mixture, as shown in Figure 2d (additional images Figure S3). AFM characterization of **H2T1** in a 4:1 chloroform/methanol solution revealed the fibrillar aggregates to have thicknesses of ∼4.5 nm (Figure 2e). The structures formed by **H2T1** in chloroform and methanol solvent mixtures are therefore quite similar to the fibrillar aggregates formed by alkyl-substituted polythiophene homopolymers in marginal solvents.[4a,14] However, a key distinction is that, in the same solvent mixture, P3HT homopolymers precipitate as large aggregates with ill-defined structures, because methanol is a very poor solvent for P3HT. Thus, the introduction of polar TEG side chains to polythiophene diblock copolymers greatly extends the range of solvent conditions under which well-defined crystalline fibrils are formed. In addition, we

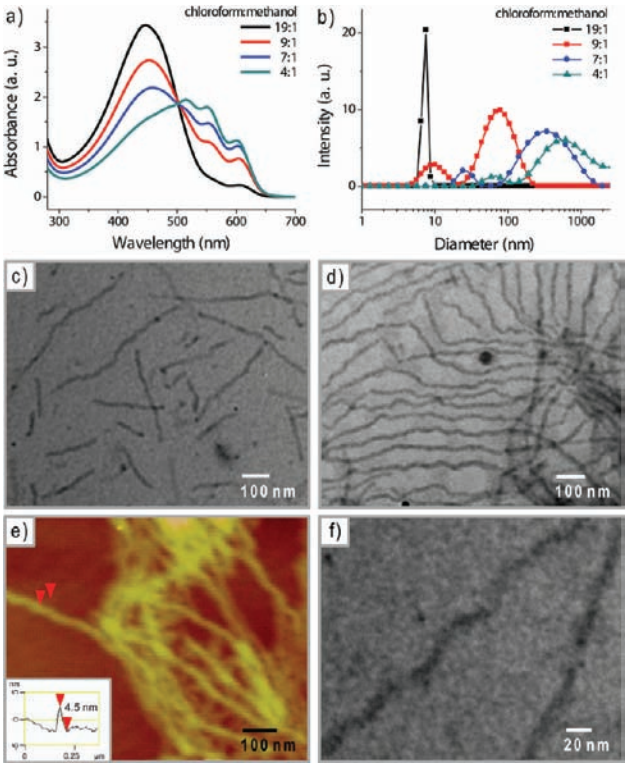

Figure 2. (a) UV−vis absorption spectra and (b) size distributions of **H2T1** from DLS for different solvent mixtures (chloroform:methanol (v/v), 1 mg/mL polymer). TEM images of self-assembled nanostructures formed in (c) 19:1 and (d) 4:1 chloroform/methanol mixtures. (e) AFM image of nanofibrils of **H2T1** with height information. (f) High-magnification TEM image suggesting coiling of **H2T1** fibrils.

noted a wavy appearance of the **H2T1** nanowires in the TEM micrographs of Figure 2d,f, with a periodicity of ∼100 nm, suggesting a natural propensity for the wires to coil.

As oligo(ethylene glycol) can complex alkali metal cations, especially potassium, these diblock copolymers offer additional opportunities to tailor nanostructure morphologies during crystallization from solution.[7c,15] Remarkably, when KI salt was added to a solution of **H2T1**, helical ribbon structures were formed, as observed by TEM. At a salt concentration of 0.47 mM, corresponding to a 2.5:1 molar ratio of K^+ to TEG chains, well-defined helical structures were formed, consisting of single nanoribbons of width 13−16 nm, coiled with a regular pitch of ∼110 nm, as seen in Figure 3a. The contrast variations along each single helix gave rise to a banded appearance that allowed left- and right-handed helices to be distinguished. As expected based on the achiral nature of the self-assembling molecules, a roughly equal mixture of left- and right-handed helices was observed; circular dichroism measurements (Figure S4) also did not reveal any preference for a particular chirality. Figure 3b shows two single-helical ribbons of the same handedness intertwining to form a double-stranded helix. After 1 day of aging in solution, predominantly multiple-stranded helical structures were observed, as seen in Figure 3c. Interestingly, the pitch of a superhelix containing *n* elementary strands was found to be *n* times the pitch of the single helical ribbons; i.e., while the single-helical fibrils repeat their structure every 110 nm, the double helices show a repeat distance of 230 nm (Figure 3b), and larger bundles show correspondingly greater pitches (Figure S5a). When the KI

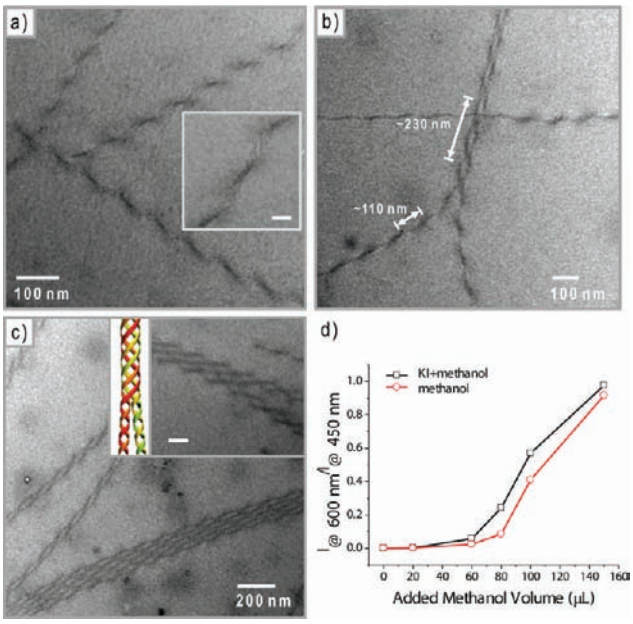

Figure 3. (a) TEM images of **H2T1** after addition of KI revealed helical ribbons with a regular pitch. Inset: magnified image (scale bar, 20 nm). TEM images showing the structural transformation of **H2T1** containing KI (0.47 mM) from (b) single- to double- and (c) multiple-stranded helices. Inset: TEM image and schematic showing association of double helices into quadruple superhelices (scale bar, 100 nm). (d) Absorption changes (monitored at 450 and 600 nm) of **H2T1** solution upon gradual addition of methanol, or 0.12 mM KI in methanol, into 200 μL of a chloroform solution of **H2T1** (0.1 mg/mL).

concentration was doubled to 0.94 mM, bundles of two or more helical strands were found after only 30 min of aging (Figure S5b).

To determine whether crystallization and salt complexation act cooperatively to drive assembly, two additional experiments were performed. First, the absorption spectra of **H2T1** in chloroform/methanol mixtures were measured, both with and without alkali metal ions. The degree of aggregation was assessed by comparing the absorption at 600 nm, correlated with the degree of interchain order,[6b,11] to that at 450 nm, characteristic of nonaggregated chains. As seen in Figure 3d, the presence of KI led to more pronounced aggregation of **H2T1** at a given methanol content, indicating that both the reduction in solvent quality and ion complexation promote aggregation of block copolymer chains into fibrils. Second, the importance of simultaneous addition of salt and poor solvent was investigated. When KI was introduced to suspensions of fibrils that had previously been prepared in chloroform/methanol mixtures, no tendency for **H2T1** to form superhelical nanowires was observed. Therefore, the observed helical assemblies do not simply reflect a salt-induced bundling of **H2T1** fibers, but instead indicate a cooperative process of crystallization and complexation.

While superhelix formation represents a common self-assembly motif for peptides,[16] block copolymers,[17] and dendrimers,[18] a unified understanding of this behavior is lacking, especially for achiral molecules. However, twisting and helical bundling in achiral systems can be understood in many cases by the introduction of attractive interactions along the periphery of slender objects. Twisting into helices allows for efficient contact between the surfaces on neighboring loops along the helix, and the competition against bending provides a preferred pitch. Such effects have been observed for multivalent ion complexation by lipid tubules[19] and block copolymer micelles[17b] and were predicted for elastic tubes in the presence of depletion attractions.[20] In the current system, K^+ ions serve as bridging sites between individual TEG side chains, leading to attractive interactions between P3(TEG)T chains (also modified by electrostatic interactions between complexed K^+ ions and associated I^- counterions). The existence of interfibril attractions is clearly seen in the formation of bundles (Figure 3b,c), and it is notable that the observed pitch varies linearly with the number of associated strands, suggesting a preferred center-to-center spacing of ~40 nm between neighboring strands in the bundle. We suspect that these salt-induced intra- and interfibril attractions compete with the bending rigidity of the fibril to set the helical pitch. However, we note that the tendency for twisting *even in the absence of salt*, as suggested by Figure 2d,f, raises an additional possible driving force associated with steric considerations due to the mismatch in packing between the P3HT and P3(TEG)T blocks. The P3(TEG)T chains at the fibril edges are more sterically demanding and better solvated than the P3HT component. These chains prefer to pack at lower areal chain density than crystalline P3HT, and this frustration can be partially relieved by twisting of the fibrils with some helicoidal character, as we illustrate in the magnified region of the schematic in Figure 1. We note that a similar mode of helical packing, i.e., a twist in the orientation of neighboring polythiophene chains along the length of the fibril, is thought to give rise to the pronounced chiroptical activities of assemblies of polythiophenes with chiral substituents.[21] In the case considered here, complexation of K^+ ions may modify the preferred packing density of P3(TEG)T, shifting the balance between stretching and bending energies that determine the helical shape of the fibril.[22]

Finally, we investigated the role of block copolymer composition in the formation of fibrils and larger aggregates by preparing **H1T1** and **H4T1** block copolymers with similar overall molecular weights but respectively longer and shorter P3(TEG)T block lengths than **H2T1** (Table 1). In 4:1 chloroform/methanol, **H1T1** formed short fibrils with widths of 14−17 nm and lengths of a few hundred nanometers (Figure 3a), while the P3HT-rich **H4T1** self-organized into long fibrils with lateral dimensions of 13−15 nm and lengths of several micrometers. The fibers of **H4T1** showed somewhat wavy structures (Figure 3b), suggesting some degree of twist, as for **H2T1**. The hydrodynamic sizes of the aggregates, determined by DLS (Figure S7), increased with decreasing P3(TEG)T content, consistent with the TEM observations in Figures 3 and 4. These behaviors can be understood in terms of the balance between repulsive interactions among the well-solvated P3(TEG)T blocks and attractive interactions driving crystallization of the P3HT block, leading to a larger driving force for assembly of polymers with greater P3HT content. Little influence of composition is found on fibril width, suggesting that the lateral dimensions are controlled by the contour lengths of fully extended block copolymer chains.[4b] Interestingly, for **H1T1** and **H4T1**, the presence of KI during crystallization did not yield the helical aggregates seen for **H2T1**. Instead, added salt induced a lengthening of **H1T1** fibers with limited aggregation of the fibrils (Figure 4c) and extensive lateral association of long **H4T1** fibers (Figure 4d). Thus, while KI promotes intra- and interfibril interactions in these polymers, the superhelical structures formed by **H2T1** apparently reflect a delicate balance of interactions between the complexed P3(TEG)T blocks and those of the crystalline P3HT blocks that is sensitive to polymer composition. Further investigation into the range of P3HT and other copolymers that are amenable to superhelix formation is underway.

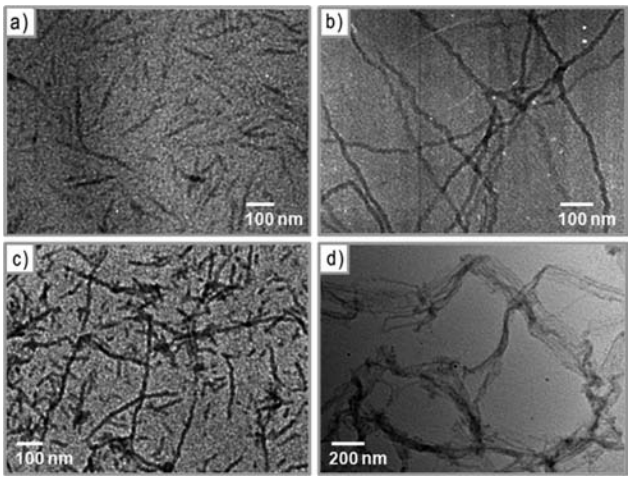

Figure 4. TEM images of (a) short fibrils of **H1T1** and (b) long twisted fibrils of **H4T1**. TEM images of (c) **H1T1** and (d) **H4T1** after addition of KI revealed the formation of longer fibrils and bundles consisting of laterally stacked fibrils, respectively.

In summary, we have described crystallization-driven assembly of conjugated P3HT-*b*-P3(TEG)T diblock copolymers, providing a large contrast in solubility between the blocks containing nonpolar hexyl and polar TEG side chains, as well as routes to modify crystallization mechanisms through interactions with the minor, polar block. These polymers efficiently assemble into well-defined fibers in the presence of the highly selective solvent methanol. Complexation of K^+ ions with the TEG side chains drives the formation of helical ribbons, which further associate into superhelical structures. Thus, P3HT-*b*-P3(TEG)T provides a novel and unique system for fundamental studies on the self-assembly of conjugated polymers, as well as new opportunities for tailoring the morphologies of materials potentially suitable for sensors and optoelectronic devices.

■ ASSOCIATED CONTENT

Supporting Information. Synthetic and other experimental details. This material is available free of charge via the Internet at http://pubs.acs.org.

■ AUTHOR INFORMATION

Corresponding Author

tsemrick@mail.pse.umass.edu; rhayward@mail.pse.umass.edu

Present Addresses

[†]Graduate School of Analytical Science and Technology, Chungnam National University, Daejeon 305-764, Republic of Korea

■ ACKNOWLEDGMENT

We are grateful to G. Grason for helpful discussions. This work was supported by the Polymer-Based Materials for Harvesting Solar Energy, an Energy Frontier Research Center funded by the U.S. Department of Energy, Office of Basic Energy Sciences, under Award No. DE-SC0001087 (support for E.L.), and the NSF-MRSEC on Polymers at UMass (DMR-0820506). Z.P. is supported by the DOE Office of Science Graduate Fellowship Program, administered by Oak Ridge Associated Universities (ORAU) under DOE contract no. DE-AC05-06OR23100.

■ REFERENCES

(1) (a) Peet, J.; Heeger, A. J.; Bazan, G. C. *Acc. Chem. Res.* **2009**, *42*, 1700–1708. (b) Brabec, C. J.; Sariciftci, N. S.; Hummelen, J. C. *Adv. Funct. Mater.* **2001**, *11*, 15–26.

(2) (a) Kline, R. J.; McGehee, M. D. *Polym. Rev.* **2006**, *46*, 27–45. (b) Osaka, I.; McCullough, R. D. *Acc. Chem. Res.* **2008**, *41*, 1202–1214. (c) Lim, J. A.; Liu, F.; Ferdous, S.; Muthukumar, M.; Briseno, A. L. *Mater. Today* **2010**, *13*, 14–24.

(3) Yang, X.; Loos, J. *Macromolecules* **2007**, *40*, 1353–1362.

(4) (a) Ihn, K. J.; Moulton, J.; Smith, P. *J. Polym. Sci., Part B: Polym. Phys.* **1993**, *31*, 735–742. (b) Liu, J.; Arif, M.; Zou, J.; Khondaker, S. I.; Zhai, L. *Macromolecules* **2009**, *42*, 9390–9393.

(5) (a) Samitsu, S.; Shimomura, T.; Heike, S.; Hashizume, T.; Ito, K. *Macromolecules* **2008**, *41*, 8000–8010. (b) Friedel, B.; Mcneill, C. R.; Greenham, N. C. *Chem. Mater.* **2010**, *22*, 3389–3398.

(6) (a) Xin, H.; Kim, F. S.; Jenekhe, S. A. *J. Am. Chem. Soc.* **2008**, *130*, 5424–5425. (b) Liu, L. G.; Lu, G. H.; Yang, X. N. *J. Mater. Chem.* **2008**, *18*, 1984–1990.

(7) (a) Wu, P.-T.; Ren, G.; Li, C.; Mezzenga, R.; Jenekhe, S. A. *Macromolecules* **2009**, *42*, 2317–2320. (b) He, M.; Zhao, L.; Wang, J.; Han, W.; Yang, Y.; Qiu, F.; Lin, Z. *ACS Nano* **2010**, *4*, 3241–3247. (c) Park, S.-J.; Kang, S.-G.; Fryd, M.; Saven, J. G.; Park, S.-J. *J. Am. Chem. Soc.* **2010**, *132*, 9931–9933.

(8) (a) Loewe, R. S.; Khersonsky, S. M.; McCullough, R. D. *Adv. Mater.* **1999**, *11*, 250–251. (b) Loewe, R. S.; Ewbank, P. C.; Liu, J.; Zhai, L.; McCullough, R. D. *Macromolecules* **2001**, *34*, 4324–4333.

(9) Moulé, A. J.; Meerholz, K. *Adv. Funct. Mater.* **2009**, *19*, 3028–3036.

(10) Yamamoto, T.; Komarudin, D.; Arai, M.; Lee, B.-L.; Suganuma, H.; Asakawa, N.; Inoue, Y.; Kubota, K.; Sasaki, S.; Fukuda, T.; Matsuda, H. *J. Am. Chem. Soc.* **1998**, *120*, 2047–2058.

(11) (a) Brown, P. J.; Thomas, D. S.; Köhler, A.; Wilson, J. S.; Kim, J.-S.; Ramsdale, C. M.; Sirringhaus, H.; Friend, R. H. *Phys. Rev. B* **2003**, *67*, 064203(1)–064203(16). (b) Rughooputh, S.; Hotta, S.; Heeger, A. J.; Wudl, F. *J. Polym. Sci., Part B: Polym. Phys.* **1987**, *25*, 1071–1078.

(12) (a) Huang, W. Y.; Huang, P. T.; Han, Y. K.; Lee, C. C.; Hsieh, T. L.; Chang, M. Y. *Macromolecules* **2008**, *41*, 7485–7489. (b) Xu, B.; Holdcroft, S. *Macromolecules* **1993**, *26*, 4457–4460.

(13) (a) Zhao, K.; Ding, Z.; Xue, L.; Han, Y. *Macromol. Rapid Commun.* **2010**, *31*, 532–538. (b) Liu, J.; Shao, S.; Wang, H.; Zhao, K.; Zue, L.; Gao, X.; Xie, Z.; Han, Y. *Org. Electron.* **2010**, *11*, 775–783.

(14) Merlo, J. A.; Frisbie, C. D. *J. Phys. Chem. B* **2004**, *108*, 19169–19179.

(15) (a) Marsella, M.; Swager, T. M. *J. Am. Chem. Soc.* **1993**, *115*, 12214–12215. (b) Lévesque, I.; Leclerc, M. *Chem. Mater.* **1996**, *8*, 2843–2849. (c) McCullough, R. D.; Williams, S. P. *Chem. Mater.* **1995**, *7*, 2001–2003.

(16) (a) Muraoka, T.; Cui, H.; Stupp, S. I. *J. Am. Chem. Soc.* **2008**, *130*, 2946–2947. (b) Murnen, H. K.; Rosales, A. M.; Jaworski, J. N.; Segalman, R. A.; Zuckermann, R. N. *J. Am. Chem. Soc.* **2010**, *132*, 16112–16119.

(17) (a) Cornelissen, J. J. L. M.; Fischer, M.; Sommerdijk, N. A. J. M.; Nolte, R. J. M. *Science* **1998**, *280*, 1427–1430. (b) Zhang, S.; Cui, H.; Chen, Z.; Wooley, K. L.; Pochan, D. J. *Soft Matter* **2008**, *4*, 90–93.

(18) (a) Enomoto, M.; Kishimura, A.; Aida, T. *J. Am. Chem. Soc.* **2001**, *123*, 5608–5609. (b) Böttcher, C.; Schade, B.; Ecker, C.; Rabe, J. P.; Shu, L.; Schlüter, A. D. *Chem. Eur. J.* **2005**, *11*, 2923–2928.

(19) Lin, K.-C.; Weis, R. M.; McConnell, H. M. *Nature* **1982**, *296*, 164–165.

(20) Snir, Y.; Kamien, R. D. *Science* **2005**, *307*, 1067.

(21) (a) Langeveld-Voss, B. M. W.; Janssen, R. A. J.; Meijer, E. W. *J. Mol. Struct.* **2000**, *521*, 385. (b) Kane-Maguire, L. A. P.; Wallace, G. G. *Chem. Soc. Rev.* **2010**, *39*, 2545.

(22) Ghafouri, R.; Bruinsma, R. *Phys. Rev. Lett.* **2005**, *94*, 138101.